Supporting Information

Novel blocker of onco SK3 channels derived from scorpion toxin tamapin and active against migration of cancer cells

*Marlen Mayorga-Flores, Aurélie Chantôme, Monserrath Melchor-Meneses, Gustavo Alfredo Titaux-Delgado, Rodrigo Galindo-Murillo, Christophe Vandier and Federico del Río-Portilla**

Table of Contents

1. EXPERIMENTAL SECTION

1.a Construction of expression plasmids

Expression of r-tam was performed on *E. coli* as previously reported.[1] Mutants were obtained by site-directed mutagenesis which was made by overlap-extension PCR (Phusion, Bio Labs, Inc.) using the r-tam plasmid as template. The oligonucleotides (SIGMA-ALDRICH) used to introduce the mutations were designed in no complementary arrangement. All the new vectors were verified by DNA sequencing (Laragen, Culver City, CA, USA) using T7 term primers.

1.b Toxin-like peptides expression and purification

Escherichia coli strain Rosetta was transformed with each plasmid expression thioredoxin system previously constructed to express all toxins mutants. Gene encoding for the fusion protein is thioredoxin–His6-LVPRGM-tamapin. Cells were grown overnight at 37 °C in Luria-Bertani medium. This was used as primary inoculum for expression in big scale (1 L) cultures. Freshly seeded cultures were grown at 37 °C. Cultures were monitored by periodic measurement of the optical density at 600 nm. Protein expression was induced by the addition of IPTG (0.5 mM final concentration) when the A600nm reached 0.6–0.8. The cultures were allowed to grow further for a period of 7 h at 37°C. The cells were then harvested by centrifugation (6000 X g, 5 min at 4 °C) and then the pelleted cells were suspended in 50 mL of lysis buffer per gram of pellet cells (20 mM Tris, pH 8.0 and 150 mM NaCl). Cell lysis was conducted by sonication using a sonicator (Misonix 3000, power level 5) and clarified by centrifugation (16000 X g, 40 min at 4°C). The soluble protein in the lysate was subject to purification by metal-chelate affinity chromatography. Soluble fraction was applied onto a Ni2+ column (Hi-Trap®, GE). The fusion protein bounded to the column was eluted with buffer containing imidazole 0.3 M. The protein of interest was dialyzed against protease cleavage buffer (50 mM Tris, 10 mM CaCl2, 200 mM NaCl, pH 8.0). The peptides were liberated from the fusion protein by hydrolysis with thrombin (Sigma-Aldrich). The reaction was carried out at room temperature for 12 h. Protein concentration was determined using the theoretical molar extinction coefficients at 280 nm and then adjusted to 1.0 mg/mL. About 20-30 mg/L of corresponding protein fusion was obtained in LB medium. The cleavage reaction was monitored by

SDS-PAGE electrophoresis and the fragments with thioredoxin and His-tag were removed by affinity chromatography to Ni2+. The sequence (LVPRGM) composing the thrombin cleavage site provides two additional amino acids (Gly and Met) to the N-terminal.

1.c Solid extraction

The fraction eluted from the affinity chromatography was concentrated, fractionated and desalted in a cartridge Strata-C18T (Phenomenex), the fraction containing the peptide eluted with 60% of acetonitrile. The protein was lyophilized.

1.d CNBr reaction

We deleted the Gly-Met residues on N-terminal with CNBr. A sample of GM-toxin was directly dissolved in trifluoroacetic acid at 50% v/v to a final concentration of 10 mg/mL. Immediately to the addition of the protein the oxygen in the solution was purged with nitrogen for 1 hour, then, 120 equivalents of cyanogen bromide were added for each methionine present in the protein sequence. Reaction was protected from light sources and stirring during 24 h under N_2 atmosphere. The reaction was stopped by adding water with a proportion of four-fold the reaction´s volume. This dissolution was diluted with distilled water until the pH was 2.0. Finally, the sample was recovered from solution by Strata C18-T cartridges and prepared for reverse phase HPLC purification.

1.e Reverse phase chromatography

Final purification was carried out by reversed phase-HPLC using a C12 analytical column at 25 °C (Phenomenex, Jupiter, 250 × 4.6 mm, 4.0 μm particle diameter, 90 Å pore size) equipped with a C12 guard column (Phenomenex, Jupiter, 10 μm), the elution was conducted at 1 mL/min, employing solutions A (water + 0.05% v/v TFA) and B (acetonitrile 0.05% v/v TFA). A linear gradient from

10% to 30% solution B was developed over 20 min. The peptide absorbance was monitored at 230 nm. The polypeptides obtained from reverse chromatography were ≥98.0 % pure and then they were analyzed by mass spectrometry. The desired fraction was lyophilized and then quantified. All peptides described in this work were successfully produced and purified using the same methodology.

1.f Mass spectrometry

The molecular masses of the purified peptides were obtained by MALDI-TOF experiments on Bruker Daltonics Microflex LT equipment. For each analysis 100 nmol of toxin were mixed with 3 μL of matrix (supersaturated solution of a-cyano-4-hydroxy-cinnamis acid in acetonitrile 60% in water added with trifluoroacetic acid at 0.05% v/v and then 1 μL of this mixture was spotted onto the MALDI plate and later analyzed. Data were acquired in the m/z range of 0−8000 Da. The reflector operation mode was used acquiring 200 shots.

1.g NMR 3D structure

Lyophilized toxin was dissolved at 3 mM in H_2O 5% (v/v) of D_2O. NMR data were acquired at 298 K employing a Varian spectrometer operating at 500 MHz proton frequencies. The TOCSY spectra were recorded with mixing times of 80 ms, and the NOESY spectra were recorded with mixing times of 150 and 300 ms. All 2D-NMR spectra were collected as 1024 data complex point matrices using 32 scans.[2] NMR data were processed using NMRpipe[3] and a shifted sine window function and zero filling was applied prior to Fourier transformation. The identification of amino acid spin systems and the sequential assignment were done using the

standard strategy described by Wüthrich.[4] The spin systems were identified in the TOCSY spectra. Sequential assignments were obtained from analysis of HN–HN, HN–Hα and HN–Hβ connectivity's in NOESY spectra. Distance constraints were derived from the two-dimensional NOESY with a mixing time of 150 ms. Secondary structure Chemical Shift Index (CSI) was calculated according to the method of Wishart and Sykes[5] for each residue based only in proton resonances. Data analysis and peak identification was performed with CARA Structure calculation. Distance and dihedral angle constraints were mainly derived from cross-peaks in NOESY. Structures were generated using CYANA, employing simulated annealing algorithms. A total of 200 structures were calculated, of which 20 structures were selected based on the CYANA target function with no constraint violations to construct the NMR structural ensemble. These 20 structures were refined using Amber 16 to represent the final solution structure. All molecular dynamics simulations and energy minimizations described here were carried out using the topology and force field parameter of AMBER-99SB. We followed one of the refinement protocols proposed by Lindorff and coworkers with few modifications.[6] Structure evaluation was performed with PROCHECK. The coordinate file of the final ensemble of all structures determined, together with the distance constraints files, were deposited in the Protein Data Bank as shown in Table 2.

1.h Molecular dynamics simulations

The channels were modeled using the sequences for SK2 (UniProt ID: Q9H2S1) and SK3 (UniProt ID: Q9UGI6), focusing on the S5-H-S6 region.

Table S.1 Sequences for SK2 and SK3 used in this work.

```
          S5 region                               H region                    S6 region
      __________________                    _____________________        ____________________
SKCa2:CPGTVLLVFSISLWIIAAWTVRACERYHDQQDVTSNFLGAMWLISITFLSIGYGDMVPNTYCGKGVCLLTGIMGAGCTALVVAVV  88
SKCa3:CPGTVLLVFSISSWIIAAWTVRVCERYHDKQEVTSNFLGAMWLISITFLSIGYGDMVPHTYCGKGVCLLTGIMGAGCTALVVAVV  88
```

Using the Swiss-model template finder tool, a search was conducted that would identify a model with the sequence of interest (table S.1) which suggested as a top result the PDB ID 2P7T with a 21.43 sequence identity score. Using UCSF-Chimera MODELLER, we adjusted the residues to match the correct sequence and an additional validation was performed by overlapping the generated models with PDB code 1BL8, which has been used in published simulations[15]. The RMSD difference between our generated models and 1BL8 is 0.63 Å and 0.64 Å for Sk2 and Sk3 respectively (considering only the heavy atoms of one of the four monomers). Both models where solvated with the TIP3P [7] water model in a truncated octahedral periodic box using the tleap module in Ambertools12. Parameters where described by the FF12SB AMBER force field.[6] An initial structural minimization was conducted starting with applying restraints on the entire solute (harmonic constant of 10 kcal/mol · $Å^2$) for 1 ns. The integration timestep was 1 fs to ensure a proper equilibration. The next step involved heating the system from 100 to 310 K using the weak-coupling thermal control. Next, the restraints where gradually lowered over 5 steps until a final equilibration simulation with no restraints was sampled for 1 ns. This initial minimization and equilibration procedure produced initial models free of clashes and structural artifacts, adequate for our present work.

Both ion channels were embedded in a full POPC membrane described by the lipid16 AMBER force field[8]. The peptide was then manually positioned at a distance of 3 Å from the center of the channel, in opposite direction of the termini residues. K^+ and Cl^- counter ions where to neutralize the system using the Joung-Cheatham ion parameters added [9]. Periodic boundary conditions were set in a triclinic cell and the water model used for explicit solvation. A careful minimization and equilibration procedure were then run applying restraints in the whole solute to allow the waters to equilibrate for 100 ps. The restraints were then gradually decreased from a value of 10 to 0.5; each step running for 500 ps. Production simulation using the NTP ensemble was run for a total of 300 ns for each system with Langevin dynamics to hold the temperature at 300 K (gamma value of 1.0, ig=-1). The integration timestep was 4 fs using the hydrogen-mass repartition scheme [10]. Each system was run a total of five independent simulations and analysis was performed aggregating the five trajectories (for a total of 1.5 μs for each system). All simulations were done using the GPU code of AMBER 16 [11,12]. All structural analysis was done using CPPTRAJ[13].

1.i Cell lines culture and SKCa channel stable transfections

Human cancer cell line MDA-MB-435s was purchased from the American Type Culture Collection (ATCC, LGC Promochem, Molsheim, France) and was grown as already described[14]. This cell line was transduced by a lentivector containing either an interfering shRNA specific to SK3 ($SK3^-$ cells) or a non-targeting shRNA ($SK3^+$ cells) as previously validated.[15] HEK 293 and HEK293T were from ATCC, maintained in Dulbecco's Modified Eagle's Medium, supplemented with 10% (v:v) fetal bovine serum (Lonza, France). Stable expression of rat SK2 channels in HEK293 cells were performed as previously described[15]. Stable expressions of human SK3

channels in HEK293T cell line were generated by transfecting cells with pPRIPu-hSK3 vector (kindly provided by Dr. P. Martin, institute de biologie Valrose, Nice, France) and by subjecting cells puromycin selection (1 mg/mL) from 48 hours post-transfection up to 20 days.

1.j Electrophysiology and cell migration assays

Experiments were performed with cells seeded into 35-mm Petri dishes at 2000 cells per cm^2. All voltage clamp experiments were performed using the conventional whole cell recording configuration of the patch clamp technique as previously described[14,16,15]. Cell migration was determined as described elsewhere[14,16].

1.k Solutions and drugs

The physiological saline solution had the following composition (in mM): NaCl 140, $MgCl_2$ 1, KCl 4, $CaCl_2$ 2, D-glucose 11.1, HEPES 10; and was adjusted to pH 7.4 with NaOH. The pipette solution for the whole-cell recordings contained (in mM): KCl 145, $MgCl_2$ 1, Mg-ATP 1, HEPES 10, $CaCl_2$ 0.87, EGTA 1 (pCa6). The pH of the solution was adjusted to 7.2 with KOH.

1.l Statistics

Data were expressed as median with quartile or mean ± SEM (N=number of experiments; *n*=number of cells). Statistical analysis was made using the unpaired Student-*t*-test or the Mann-Whitney test when normality tests. For comparison between more than two means, we used Kruskal-Wallis one-way analysis of variance followed by Dunn's test. Differences were considered significant when $p<0.05$. Statistical analysis was performed using GraphPad Prism 6.

2. NMR structure statistics

Table S.2. NMR structure statistics.

NMR and Ramachandran statistics for all the peptides in this work.

	Y31+N	ΔP30	ΔP30/Y31+N	E25K	K27E	E25K/K27E	Y31H	Y31A	E25A	K27A	K20E
NMR statistics											
Total	402	351	406	366	394	400	375	330	403	407	427
Short range	309	262	298	281	279	270	277	254	281	289	292
Medium range	51	42	55	46	61	69	52	41	63	57	68
Long range	42	47	53	39	54	61	46	35	59	61	67
Average target function value	0.02	0.00	0.00	0.04	0.02	0.00	0.02	0.02	0.02	0.02	0.02
Average backbone RMSD to mean	0.50	0.42	0.39	0.54	0.50	0.39	0.39	0.64	0.35	0.56	0.35
Average heavy atom RMDS to mean	1.17	1.07	0.95	1.28	1.13	1.10	1.06	1.22	0.99	1.11	1.03
Ramachandran statistics											
Most favored regions	87.1%	87.2%	74.6%	83.2%	84.6%	81.4%	81.6%	82.2%	88.2%	78.8%	89.4%
Additionally allowed regions	12.9%	12.8%	25.4%	16.8%	15.4%	18.6%	18.4%	17.8%	11.8%	21.2%	10.6%
Generously allowed regions	0.0%	0.0%	0.0%	0.0%	0.0%	0.0%	0.0%	0.0%	0.0%	0.0%	0.0%
Disallowed regions	0.0%	0.0%	0.0%	0.0%	0.0%	0.0%	0.0%	0.0%	0.0%	0.0%	0.0%

Figure S.1. 1H-NMR spectra at 500 MHz of A) Y31A and B) K20A. Proton signals at 9.87, 9.83 and 5.75 ppm are characteristics of a folded tamapin mutant.

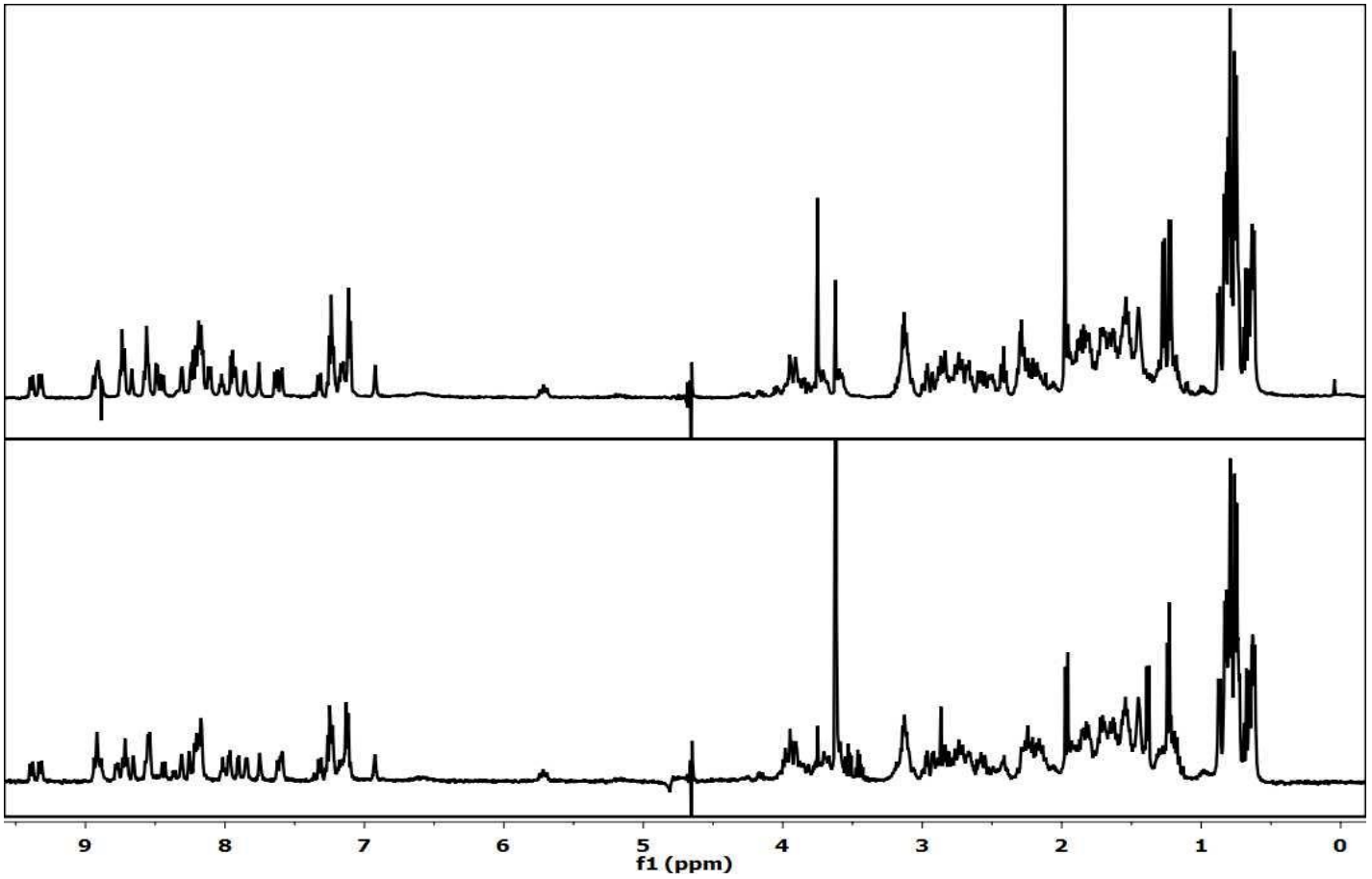

Figure S.2. Finger print region of a 500 MHz NOESY spectra at 300 ms mixing time and DPFGSE water suppression of K25E mutant.

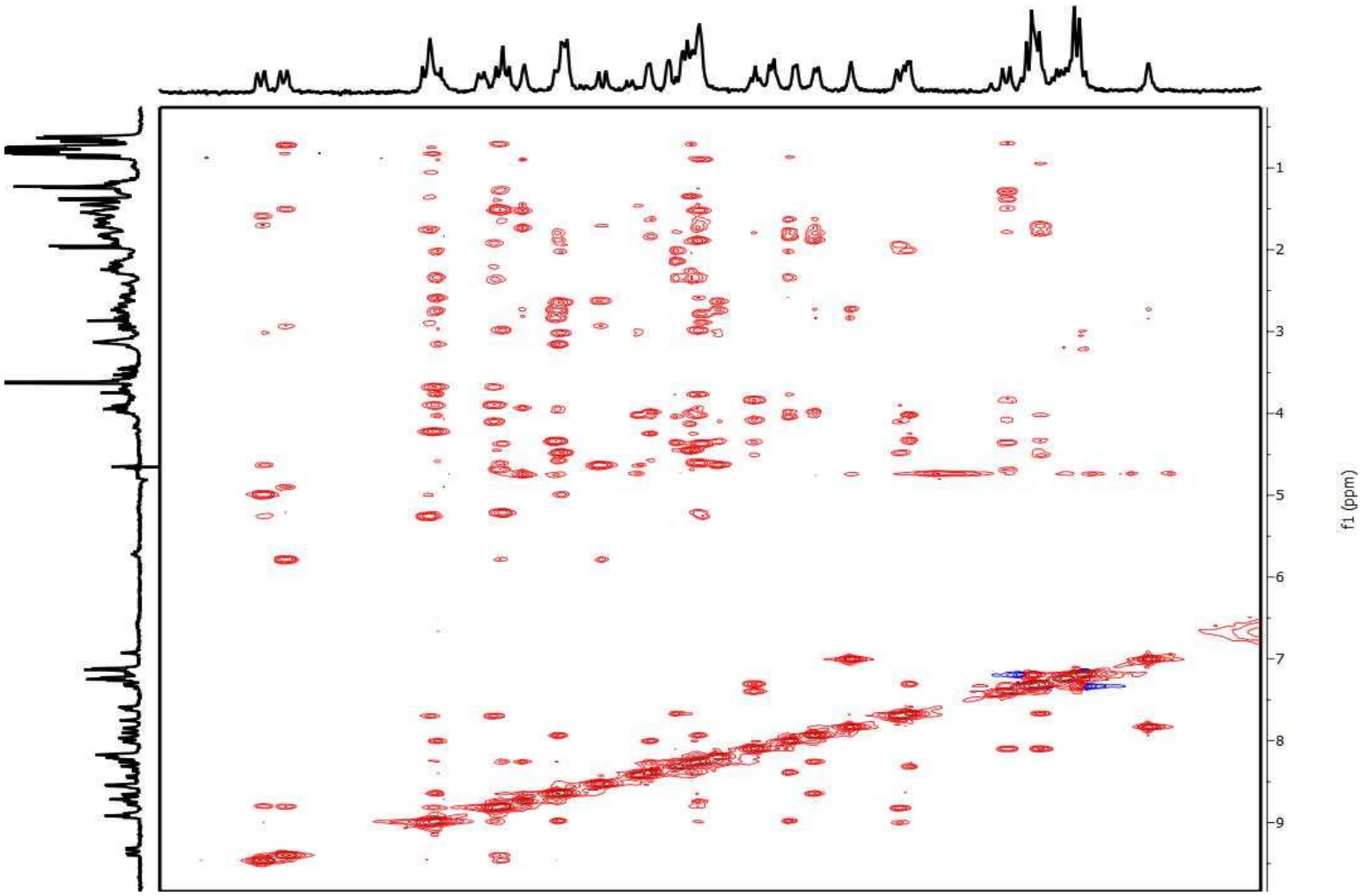

Figure S.3. Disulfide bridges by 2D-NOESY A) r-tamapin and B) E25K/K27E mutant.

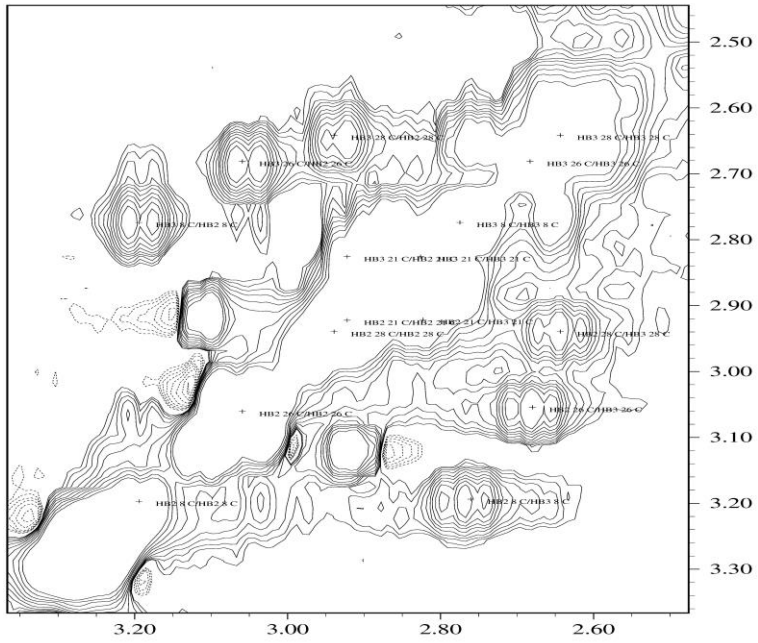

References

(1) Ramírez-Cordero, B.; Toledano, Y.; Cano-Sánchez, P.; Hernández-López, R.; Flores-Solis, D.; Saucedo-Yáñez, A. L.; Chávez-Uribe, I.; Brieba, L. G.; Del Río-Portilla, F. Cytotoxicity of Recombinant Tamapin and Related Toxin-like Peptides on Model Cell Lines. *Chemical Research in Toxicology* **2014**, *27* (6), 960–967. https://doi.org/10.1021/tx4004193.

(2) Flores-Solis, D.; Toledano, Y.; Rodríguez-Lima, O.; Cano-Sánchez, P.; Ramírez-Cordero, B. E.; Landa, A.; Rodríguez de la Vega, R. C.; del Rio-Portilla, F. Solution Structure and Antiparasitic Activity of Scorpine-like Peptides from Hoffmannihadrurus Gertschi. *FEBS Letters* **2016**, *590*, 2286–2296. https://doi.org/10.1002/1873-3468.12255.

(3) Diseases, K.; Bay, C. W.; Kong, H. NMRPipe : A Multidimensional Spectral Processing System Based on UNIX Pipes *. **1995**, *6*, 277–293.

(4) Simpson, P. J. *NMR of Proteins and Nucleic Acids*, 1st Ed.; A Wiley-Interscience Publication, 2015; Vol. 44. https://doi.org/10.139/9781782622758-00348.

(5) Wishart, D. S.; Sykes, B. D.; Richards, F. M. The Chemical Shift Index: A Fast and Simple Method for the Assignment of Protein Secondary Structure through NMR Spectroscopy. *Biochemistry* **1992**, *31* (6), 1647–1651. https://doi.org/10.1021/bi00121a010.

(6) Lindorff-Larsen, K.; Piana, S.; Palmo, K.; Maragakis, P.; Klepeis, J. L.; Dror, R. O.; Shaw, D. E. Improved Side-Chain Torsion Potentials for the Amber Ff99SB Protein Force Field. *Proteins* **2010**, *78* (8), 1950–1958. https://doi.org/10.1002/prot.22711.

(7) Jorgensen, W. L.; Chandrasekhar, J.; Madura, J. D.; Impey, R. W.; Klein, M. L. Comparison of Simple Potential Functions for Simulating Liquid Water. *Journal of Chemical Physics* **1983**, *79* (2), 926. https://doi.org/10.1063/1.445869.

(8) Dickson, C. J.; Madej, B. D.; Skjevik, Å. A.; Betz, R. M.; Teigen, K.; Gould, I. R.; Walker, R. C. Lipid14: The Amber Lipid Force Field. *Journal of Chemical Theory and Computation* **2014**, *10* (2), 865–879. https://doi.org/10.1021/ct4010307.

(9) Joung, I. S.; Cheatham 3rd, T. E. Determination of Alkali and Halide Monovalent Ion Parameters for Use in Explicitly Solvated Biomolecular Simulations. *The Journal of Physical Chemistry B* **2008**, *112*, 9020–9041. https://doi.org/10.1021/jp8001614.

(10) Hopkins, C. W.; Le Grand, S.; Walker, R. C.; Roitberg, A. E. Long Time Step Molecular Dynamics through Hydrogen Mass Repartitioning. *Journal of Chemical Theory and Computation* **2015**, *11* (4), 1864–1874. https://doi.org/10.1021/ct5010406.

(11) Götz, A. W.; Williamson, M. J.; Xu, D.; Poole, D.; Le Grand, S.; Walker, R. C. Routine Microsecond Molecular Dynamics Simulations with AMBER on GPUs. 1. Generalized Born. *Journal of chemical theory and computation* **2012**, *8* (5), 1542–1555. https://doi.org/10.1021/ct200909j.

(12) Salomon-Ferrer, R.; Götz, A. W.; Poole, D.; Grand, S. Le; Walker, R. C.; Le Grand, S.; Walker, R. C. Routine Microsecond Molecular Dynamics Simulations with AMBER on GPUs. 2. Explicit Solvent Particle Mesh Ewald. *Journal of Chemical Theory and Computation* **2013**, *9* (9), 3878–3888. https://doi.org/10.1021/ct400314y.

(13) Roe, D. R.; Cheatham 3rd, T. E. PTRAJ and CPPTRAJ: Software for Processing and Analysis of Molecular Dynamics Trajectory Data. *Journal of Chemical Theory and Computation* **2013**, *9* (7), 3084–3095. https://doi.org/10.1021/ct400341p.

(14) Potier, M.; Joulin, V.; Roger, S.; Besson, P.; Jourdan, M. L.; LeGuennec, J. Y.; Bougnoux, P.; Vandier, C. Identification of SK3 Channel as a New Mediator of Breast Cancer Cell Migration. *Molecular Cancer Therapeutics* **2006**, *5* (11), 2946–2953. https://doi.org/10.1158/1535-7163.MCT-06-0194.

(15) Girault, A.; Haelters, J.-P.; Potier-Cartereau, M.; Chantome, A.; Pinault, M.; Marionneau-Lambot, S.; Oullier, T.; Simon, G.; Couthon-Gourves, H.; Jaffres, P.-A.; et al. New Alkyl-Lipid Blockers of SK3 Channels Reduce Cancer Cell Migration and Occurrence of Metastasis. *Current Cancer Drug Targets* **2011**, *19*, 697–713. https://doi.org/10.2174/156800911798073069.

(16) Chantome, A.; Girault, A.; Potier, M.; Collin, C.; Vaudin, P.; Pagès, J. C.; Vandier, C.; Joulin, V. KCa2.3 Channel-Dependent Hyperpolarization Increases Melanoma Cell Motility. *Experimental Cell Research* **2009**, *315* (20), 3620–3630. https://doi.org/10.1016/j.yexcr.2009.07.021.